DMD Fast Forward. Published on November 8, 2019 as DOI: 10.1124/dmd.119.089508
This article has not been copyedited and formatted. The final version may differ from this version.

Title Page

NRF2-independent regulation of intestinal CAR by the pro-oxidant's cadmium and isothiocyanate in *hUGT1* mice

Miles Paszek[1] and Robert H. Tukey[2]

Laboratory of Environmental Toxicology, Department of Chemistry and Biochemistry[1] and the Department of Pharmacology[2], University of California, San Diego, 9500 Gilman Drive, La Jolla, California 92093

DMD Fast Forward. Published on November 8, 2019 as DOI: 10.1124/dmd.119.089508
This article has not been copyedited and formatted. The final version may differ from this version.

Running Title Page

NRF2-independent regulation of DMEs by cadmium and ITCs

Corresponding author:

Robert H. Tukey, Department of Pharmacology, University of California San Diego, 9500 Gilman Drive, La Jolla, California 92093-0722.

Email: rtukey@ucsd.edu

Abstract: 222

Introduction: 590

Discussion: 969

Abbreviations: CAR, constitutive androstane receptor; CCRP, cytoplasmic car retention protein; CYP, cytochrome P450; ERK1/2, extracellular signal-regulated kinases 1 and 2; HSP70/90, heat shock proteins 70 and 90; KEAP1, Kelch-like ECH associated protein 1; NRF2, nuclear factor, erythroid 2 like 2; P38, mitogen-activated protein kinase 11; TSB, total serum bilirubin

DMD Fast Forward. Published on November 8, 2019 as DOI: 10.1124/dmd.119.089508
This article has not been copyedited and formatted. The final version may differ from this version.

Abstract

Environmental toxicants such as heavy metals from contaminated water or soil and isothiocyanates (ITC) from dietary sources act as pro-oxidants by directly generating reactive oxygens species (ROS) or through depleting cellular antioxidants such as glutathione. Toxicants can alter drug metabolism and it was reported that CYP2B10 and UGT1A1 are induced by phenethyl isothiocyanate (PEITC) through the constitutive androstane receptor (CAR). The possibility that NRF2, the master regulator of the antioxidant response, could co-activate CAR was investigated in neonatal *hUGT1/Nrf2*$^{-/-}$ mice. Neonatal mice were treated with PEITC or cadmium (Cd^{2+}) by oral gavage for two days. Both PEITC and Cd^{2+} induced UGT1A1 RNA and protein in intestinal tissues in both *hUGT1/Nrf2*$^{+/-}$ and *hUGT1/Nrf2*$^{-/-}$ neonates, indicating NRF2-independent regulation of UGT1A1. Increases in CYP2B10 RNA in intestinal tissues were observed following PEITC or Cd^{2+} exposure. Activation of intestinal CAR by Cd^{2+} exposure was directly assessed by nuclear fractionation and Western blot analyses at 0.5, 1, 2, and 4 hours after treatment in *hUGT1* neonates and after 48 hours in *hUGT1/Nrf2*$^{+/-}$ and *hUGT1/Nrf2*$^{-/-}$ neonates. CAR localized to the nucleus independent of NRF2 48 hours after exposure. Substantial CAR localization to the nucleus occurred at the 2- and 4-hour time points, coinciding with a decrease in cytoplasmic ERK1/2 phosphorylation and a nuclear increase in P38/p-P38 content. This suggests a novel oxidative stress-MAPK-CAR axis exists with phenotypic consequences.

Significance Statement

Pro-oxidant toxicants can alter drug metabolism through activation of CAR, independent of the NRF2-KEAP1 signaling pathway. The changes in proteins associated with drug metabolism are likely mediated through an oxidative stress-MAPK-CAR axis that have been linked to increases in intestinal maturation.

Introduction

Exposure to certain environmental toxicants is capable of altering drug metabolism through the activation of selective transcription factors, such as xenobiotic and nuclear receptors (XRs and NRs). The activation of XRs and NRs typically occurs through direct ligand binding to the receptor or through post translation modifications. In vitro models enable medium- to high- throughput screening of compounds abilities to activate nuclear receptors while in vivo models provide more complex details such as absorption, elimination, and tissue specific metabolism.

An in vivo model that lends itself well to reverse genetic approaches is the humanized *UDP-glucuronosyltransferase 1* (*hUGT1*) mouse model due to the readily quantifiable phenotype that changes following XR or NR activation (Fujiwara et al., 2010; Chen and Tukey, 2018). The phenotype is presented as neonatal hyperbilirubinemia, a condition unique to humans in which increased turnover of red blood cells causes heme degradation to bilirubin which, accumulates systemically (Pearson, 1967). The accumulation of bilirubin occurs because hepatic expression of UGT1A1, the only enzyme capable of conjugating bilirubin for excretion (Bosma et al., 1994), is developmentally delayed at the transcriptional level (Burchell et al., 1989). However, we have demonstrated that control of intestinal UGT1A1 during development plays a key role in the clearance of serum bilirubin during the neonatal period (Fujiwara et al., 2010; Liu et al., 2016; Chen et al., 2017). Induction of the *UGT1A1* gene in *hUGT1* mice can be mediated by multiple XRs and NRs, such as the pregnane X-receptor (PXR) (Chen et al., 2012), constitutive androstane receptor (CAR) (Sugatani et al., 2001), peroxisome proliferator-activated receptor α (PPARα) (Senekeo-Effenberger et al., 2007), as well as

environmental toxicant sensors such as the aryl hydrocarbon receptor (AhR) (Yueh et al., 2005; Bonzo et al., 2007), and the nuclear factor erythroid 2-related factor 2 (NRF2) (Yueh and Tukey, 2007). Following exposure, activation of one or more of these XRs and NRs induces *UGT1A1* gene expression resulting in a reduction of total serum bilirubin (TSB) levels in *hUGT1* mice (Yueh et al., 2017; Chen and Tukey, 2018). Known transcriptional targets can be examined to determine which XR or NR is inducing *UGT1A1*, for example CAR induces the *Cyp2b10* (Honkakoski et al., 1996) gene while activated NRF2 can induce genes such as *Gsta1/2* (McMahon et al., 2001), which are sensitive to oxidative stress. The receptor mediated induction of *UGT1A1* can be confirmed in neonatal *hUGT1* mice that express a null allele for the *XR- or NRs,* where elevated TSB levels following exposure can be directly linked to a dependency on the deleted receptor (Chen et al., 2013; Liu et al., 2016; Yoda et al., 2017).

Recently, it was reported that the dietary pro-oxidants isothiocyanates (ITCs) induce hepatic UGT1A1 in a CAR-dependent fashion (Yoda et al., 2017). This is significant because the mechanisms of direct and indirect activation of CAR are well characterized (Yoshinari et al., 2003; Osabe and Negishi, 2011; Mutoh et al., 2013; Timsit and Negishi, 2014) but have never directly implicated oxidative stress as a CAR activator. Additionally, other environmentally relevant toxicants, such as cadmium (Cd^{2+}) and arsenic (As^{3+}) that increase reactive oxygen species (ROS) have been reported to induce intestinal *Cyp2b10* and *UGT1A1* gene expression in *hUGT1* mice (Fujiwara et al., 2010; Yoda et al., 2017). However, *UGT1A1* induction by pro-oxidants has been linked to NRF2 (Yueh and Tukey, 2007), the master regulator of the antioxidant response (Moi et al., 1994). The induction mechanism of intestinal UGT1A1 in *hUGT1* mice by agents such as

Cd^{2+} and ITCs are examined with respect to their link towards activation of NRF2 and CAR.

Materials & Methods

Animal Studies.

All animals were housed at the University of California San Diego Animal Care Facility with access to food and water ad libitum. All animal use including experimental procedures, handling, and protocols were approved by the UCSD Animal Care and Use Committee (IACUC) and adhere to the National Institute of Health Guide for the Care and Use of Laboratory Animals. UCSD's Animal Care Program is accredited by the Association for the Assessment and Accreditation of Laboratory Animal Care (AAALAC). Humanized *UGT1* (*hUGT1*) mice were previously generated as described. *Nrf2*$^{-/-}$ mice were purchased from Jackson Laboratory (Stock No: 017009), and *hUGT1/Nrf2*$^{+/-}$ mice were generated and crossed for comparison to *hUGT1/Nrf2*$^{+/+}$ mice, utilizing both males and females. Additional studies involved breeding *hUGT1/Nrf2*$^{+/-}$ with *hUGT1/Nrf2*$^{-/-}$ to generate male and female mice used for neonatal studies. Neonates were treated on day 10 and 11 with $CdCl_2 \cdot 2\ ½\ H_2O$ (Cd^{2+}) or $NaAsO_2$ (As^{3+}) (Sigma-Aldrich) at 10mg/kg or PEITC (Sigma Aldrich) at 200 mg/kg by oral gavage or with water or corn oil (5µL/g bw) for vehicle control. The dosages for $CdCl_2$ and PEITC treatments were selected from dose-response curves where both the greatest reduction in total serum bilirubin levels and no observable behavioral or gross anatomical phenotypes of toxicity were obtained. Animals were anesthetized with isoflurane and euthanized by cervical dislocation.

Real-time PCR.

Intestines were collected and briefly washed with ice cold PBS 3 times before snap freezing in liquid nitrogen. Livers were collected and washed once with ice cold PBS before snap freezing in liquid nitrogen. RNA was extracted with TRIzol™ Reagent

(ThermoFisher Scientific) as described by the manufacturer's protocol. cDNA was synthesized using iScript™ cDNA Synthesis Kit (Bio-Rad) according to the manufacturer's protocol. Real-time PCR was performed using a CFX96™ Real-Time PCR Detection system (Bio-Rad) and SSoAdvanced™ Universal SYBR® Green Supermix (Bio-Rad) as described by the manufacturer's protocol. All values represent independent biological replicates and technical singlets as analyzed by the ΔΔCT method. Primers utilized for real time PCR analysis of selected genes can be found in Table 1.

Western Blot Analysis.

Whole lysate was obtained from homogenization of pulverized intestinal tissues in RIPA buffer (Millipore Sigma Cat. No. 20-188) containing protease (ThermoFisher Scientific™ Cat. No. 78429) and phosphatase (ThermoFisher Scientific™ Cat. No. 78420) inhibitors. Pulverized tissues in lysis buffer (1:4 wt/vol) were blade homogenized and incubated on ice for 15 min before centrifugation (10,000xg, 4°C, 20 min) and supernatant storage at -80°C.

Nuclear fractionation used a two-buffer extraction. Buffer A contained 10mM HEPES, 1.5 mM $MgCl_2$, 10 mM KCl, 0.5 mM DTT, and 0.05% Igepal at pH 7.9 with protease and phosphatase inhibitors. Buffer B contained 5mM HEPES, 1.5mM $MgCl_2$, 0.2 mM EDTA, 0.5 mM DTT, and 26% glycerol (v/v) at pH 7.9 with protease and phosphatase inhibitors. Pulverized tissues were homogenized in buffer A (1:4 wt:vol) using a Potter-Elvehjem homogenizer for 10 passes. Homogenates were incubated on ice for 10 minutes prior to centrifugation (1500 x g, 4°C, 10 min). The supernatant containing the cytosol was stored at -80°C. The pellet containing the nuclear contents was washed with 200 uL of buffer A before resuspension in 400 uL of Buffer B. After

resuspension, NaCl was added to a final concentration of 300mM and the solution was sonicated for 5 sec and this repeated three times. Samples were incubated on ice for 30 minutes before centrifugation (21,000xg, 4°C, 20 min). The supernatant containing the nuclear fraction was stored at -80°C. Protein concentration was determined *via* Bradford assay (Bio-Rad), and BSA (New England BioLabs) protein standards were created for simple linear regressions.

Samples were run on NuPAGE™ 4-12% Bis-Tris Protein Gels (Invitrogen) before transferring to PVDF membranes. Membranes were blocked with 5% nonfat milk or BSA for phospho-antibodies in TBST and incubated with primary antibodies overnight at 4°C and secondary antibodies for 1 hour at RT. Imaging was performed on a ChemiDoc™ Touch imaging system (Bio-Rad) using Clarity™ Western ECL substrate (Bio-Rad). All antibodies used for protein expression and localization analyses can be found in Table 2. All samples represent biological replicates and technical singlets.

Bilirubin measurement.

Approximately 50 µL of blood was obtained from the submandibular vein. Blood was centrifuged for 2 minutes at 16,000 x g and the supernatant was measured using a Unistat Bilirubinometer (Reichert Inc.) to determine total serum bilirubin (TSB) levels.

Statistical analysis

All statistical analyses were performed using GraphPad Prism's (V 6.07) two-way ANOVA with multiple comparisons. Averages +/- SEM are shown. Differences were considered statistically significant when $p<0.05$. Statistical significance is represented by the following: * $p<0.05$, ** $p<0.01$, *** $p<0.001$, **** $p<0.0001$.

DMD Fast Forward. Published on November 8, 2019 as DOI: 10.1124/dmd.119.089508
This article has not been copyedited and formatted. The final version may differ from this version.

Results

Cd^{2+} treatment induces oxidative stress markers in an NRF2-dependent manner

Intestinal tissues were collected from *hUGT1/Nrf2*$^{+/+}$, *hUGT1/Nrf2*$^{+/-}$, and *hUGT1/Nrf2*$^{-/-}$ neonates treated orally with 10mg/kg Cd^{2+} and gene targets known to be induced by NRF2 in response to oxidative stress examined by RT-qPCR (**Fig 1**). Statistically significant inductions were detected in Cd^{2+} exposed *hUGT1/Nrf2*$^{+/+}$ and *hUGT1/Nrf2*$^{+/-}$ neonates for *Nqo1* (2.7- and 1.7-fold), *Ho-1* (6.8- and 4.3-fold), *Gsta1* (37.8- and 33.0-fold), *Gsta2* (9.3- and 7.9-fold), and *Gstm3* (15.8- and 8.7-fold) genes. A gene dosage effect comparing responses between *hUGT1* and *hUGT1/Nrf2*$^{+/-}$ neonatal mice was observed for the induction of the *Nqo1*, *Ho-1*, and *Gstm3* genes. This indicates haploinsufficiency related to NRF2's induction of antioxidant response genes. When we examined the induction of these genes in *hUGT1/Nrf2*$^{-/-}$ mice following Cd^{2+} treatment, there was no statistically significant difference from the vehicle treatment of *hUGT1* mice, confirming that the induction of these genes in the gastrointestinal tract originates from the generation of ROS in the intestines. With oral Cd^{2+} treatment, there was no induction of these genes in hepatic tissue.

Cd^{2+} induces intestinal UGT1A1 and lowers TSB levels in an NRF2 independent fashion.

It was previously determined that oral Cd^{2+} treatment to neonatal *hUGT1* mice led to the induction of intestinal UGT1A1 (Liu et al., 2016). To determine if induction of the intestinal *UGT1A1* gene by Cd^{2+} was dependent upon the generation of ROS and activation of the NRF2-KEAP1 pathway, *hUGT1/Nrf2*$^{+/-}$ mice were mated and 10-day old

DMD Fast Forward. Published on November 8, 2019 as DOI: 10.1124/dmd.119.089508
This article has not been copyedited and formatted. The final version may differ from this version.

newborns treated with 10mg/kg Cd^{2+} or water by oral gavage once per day for two days before collecting blood and intestinal tissue. With *hUGT1*, *hUGT1/Nrf2*$^{+/-}$, and *hUGT1/Nrf2*$^{-/-}$ mice, Cd^{2+} treatment eliminated circulating TSB levels within two days, indicating that a mechanism had been activated to induce intestinal UGT1A1 (**Fig. 2A**). Similar reductions were observed for PEITC and As^{3+} treated neonatal mice (**Fig. S1**). Analysis of UGT1A1 expression both at the gene and protein level firmly establish that Cd^{2+} exposure induces intestinal UGT1A1 (Fig. 2B and C). Unlike the Cd^{2+} initiated induction of the *Nqo1*, *Ho-1*, *Gsta1*, *Gsta2,* and *Gstm3* genes (**Fig. 1**), which are dependent upon NRF2, induction of the intestinal *UGT1A1* gene by Cd^{2+} is not linked to the NRF2-KEAP1 pathway. It should be noted that an antioxidant-response element (ARE) has previously been identified flanking the *UGT1A1* gene in the phenobarbital-response enhancer module region (PBREM), and has been demonstrated to bind the antioxidant *tert*-butylhydroquinone (tBHQ) inducible NRF2 in treated HepG2 cells (Yueh and Tukey, 2007). In addition, the intraperitoneal administration of tBHQ to adult *TgUGT1* mice led to induction of intestinal UGT1A1, implicating the NRF2-KEAP1 pathway as a regulator of the *UGT1A1* gene (Yueh and Tukey, 2007). However, the oral administration of Cd^{2+} and induction of intestinal UGT1A1 in *hUGT1* neonatal mice does not require NRF2-KEAP1 signaling.

Intestinal *Cyp2b10* is positively regulated by Cd^{2+} exposure and induces nuclear accumulation of CAR

The nuclear receptors that induce *UGT1A1* were examined for activation by RT-qPCR analysis of their known target genes (**Fig. S2**). Only *Cyp2b10* was substantially

induced by Cd^{2+} in *hUGT1/Nrf2*$^{+/+}$ (8.4-fold), *hUGT1/Nrf2*$^{+/-}$ (13.5-fold), and *hUGT1/Nrf2*$^{-/-}$ (9.8-fold) neonates, however only heterozygotes reached statistical significance (**Fig. 3A**). Furthermore, Western blot analysis of CYP2B10 was inconclusive with no apparent detection in either vehicle or Cd^{2+} treated mice. Given that basal expression of CYP2B10 in neonatal intestinal tissue is low, CAR activation was assayed more directly via nuclear localization.

Intestinal tissues taken from *hUGT1/Nrf2*$^{+/-}$ and *hUGT1/Nrf2*$^{-/-}$ neonates exposed to Cd^{2+} were fractionated and examined for nuclear CAR accumulation by Western blot analysis (**Fig. 3B**). There was a statistically significant increase in the nuclear accumulation of CAR in *hUGT1/Nrf2*$^{+/-}$ (3.7-fold) and in *hUGT1/Nrf2*$^{-/-}$ mice (1.8-fold) following exposure to Cd^{2+}. This localization can occur independently of NRF2 but is 2-fold less in *hUGT1/Nrf2*$^{-/-}$ compared to *hUGT1/Nrf2*$^{+/-}$ neonatal mice. This indicates that NRF2 is not responsible for the activation of CAR by Cd^{2+}.

In vivo Cd^{2+} exposure induces mitogen-activated protein kinase (MAPK) phosphorylation and CAR localization

The regulation of CAR localization makes use of ERK1/2 and P38 phosphorylation, which was examined by Western blot analysis. Neonatal *hUGT1* mice were treated orally with a single dose of Cd^{2+} (10mg/kg) or water and intestinal tissues were collected 30 minutes, 60 minutes, 120 minutes, and 240 minutes after exposure. Following treatment, the neonatal mice experienced dramatic changes in MAPK phosphorylation, where a large increase in cytoplasmic phosphorylated ERK1/2 occurs in intestinal tissue between 0 and 30 minutes after oral treatment before decaying (**Fig. 4B**). Additionally, there is an

DMD Fast Forward. Published on November 8, 2019 as DOI: 10.1124/dmd.119.089508
This article has not been copyedited and formatted. The final version may differ from this version.

accumulation of P38 and phosphorylated-P38 in the nucleus (**Fig. 4A**). Similar phosphorylation patterns were observed in adult mice (data not shown). Consistent increases in CAR accumulation in the nucleus were observed in neonatal mice after 2 hours (**Fig. 4C**) coinciding with the dephosphorylation of ERK1/2 and the nuclear accumulation of P38. The observed changes in MAPK activation are consistent with known regulatory mechanisms for CAR by ERK (Koike et al., 2007) and P38 (Hori et al., 2016), supporting the observation that Cd^{2+} exposure activates intestinal CAR. The increased oxidative state following Cd^{2+} treatment, the activation of MAPK pathways, and the commensurate nuclear accumulation of CAR underlies the induction of intestinal UGT1A1.

PEITC induction of UGT1A1 retains CAR-dependency pattern in *hUGT1/Nrf2$^{-/-}$* mice.

The observation of CAR-dependent regulation of hepatic UGT1A1 by pro-oxidants was observed using neonatal *hUGT1/Car$^{-/-}$* mice treated with PEITC (Yoda et al., 2017). The tissue-specific induction patterns of hepatic and intestinal *UGT1A1* and *Cyp2b10* genes were observed in the *hUGT1/Nrf2$^{-/-}$* neonatal mice. The increased clearance of bilirubin in neonates treated with PEITC occurred concomitantly with increases in liver and intestinal expression of *UGT1A1* and *Cyp2b10* (**Fig 5**).The inducibility of intestinal *UGT1A1* by PEITC was reduced in *hUGT1/Nrf2$^{-/-}$* (16.2-fold) mice compared to *hUGT1/Nrf2$^{+/-}$* mice (30.3-fold) (**Fig 5**). No difference was observed in liver *UGT1A1* induction between *hUGT1/Nrf2$^{+/-}$* and *hUGT1/Nrf2$^{-/-}$* neonates and the induction of *Cyp2b10* was greatest in the liver (**Fig 5**). These observations are consistent with the

previous report on CAR-dependency of hepatic *UGT1A1* induction and CAR-independent intestinal *UGT1A1* induction by PEITC (Yoda et al., 2017).

DMD Fast Forward. Published on November 8, 2019 as DOI: 10.1124/dmd.119.089508
This article has not been copyedited and formatted. The final version may differ from this version.

Discussion

It has been previously demonstrated that ITCs are capable of CAR-dependent induction of liver UGT1A1 (Yoda et al., 2017). It is well-established that NRF2 is the master regulator of the antioxidant response and can induce UGT1A1 (Yueh and Tukey, 2007). Nuclear receptors are susceptible to high levels of mutual regulation (Ratman et al., 2013) from shared protein interaction partners or through binding interactions at regulatory elements, therefore it was hypothesized that oxidative stress could be co-activating CAR through NRF2. The role of oxidative stress in the regulation of NRF2 and CAR target genes in *hUGT1/Nrf2*$^{-/-}$ mice was investigated. As anticipated, NRF2-deficient mice do not generate the antioxidant response when challenged with Cd^{2+}. However, the *hUGT1/Nrf2*$^{+/-}$ mice exhibited a diminished antioxidant response in comparison to WT mice, suggesting haploinsufficiency.

By breeding *Nrf2*$^{-/-}$ mice with *hUGT1* mice, pro-oxidants could be screened for their ability to reduce TSB levels and examine the impact of this action in an NRF2-dependent fashion. The NRF2-KEAP1 pathway is not required for Cd^{2+} cadmium and ITCs to induce intestinal UGT1A1 in *hUGT1* mice to reduce TSB levels. This supports the hypothesis that CAR can be activated by oxidative stress (Yoda et al., 2017). In analysis of NR activity, we observed suppression of target genes for PXR and PPARα and slight induction of the AhR target gene, *Cyp1a1,* in WT mice (**Fig. S1**). The reason for the suppression is unclear, but the latter induction could have resulted from co-regulation of *Cyp1a1* by NRF2 and the AhR (Shin et al., 2007). The loss of this induction in the heterozygous mice can be linked to haploinsufficiency of NRF2, and there was little change in the *Nrf2*$^{-/-}$ mice. From the examined NRs, there was evidence for CAR's

DMD Fast Forward. Published on November 8, 2019 as DOI: 10.1124/dmd.119.089508
This article has not been copyedited and formatted. The final version may differ from this version.

activation from induction of the *Cyp2b10* gene. Attempts were made to confirm protein induction of CYP2B10, but the expression levels were too low for detection. Subsequently, CAR's activation was assayed more directly. In the absence of a readily available antibody for phosphorylated CAR, fractionated intestinal samples from neonates treated with Cd^{2+} were analyzed for CAR nuclear localization. After an acute cadmium exposure, CAR localized to the nucleus in an NRF2-independent manner, which indicates that co-activation of CAR by NRF2 is not responsible for the induction of intestinal UGT1A1 and the reduction of TSB levels.

The increase in ERK1/2 phosphorylation is a confounding factor in the mechanism of CAR's activation, given that p-ERK1/2 inhibits the activation of p-Thr38-CAR, keeping it sequestered in the cytoplasm (Osabe and Negishi, 2011). However, in cardiac ventricular myocytes, it has been reported that ERK1/2 can be dephosphorylated by PP2A activity that is dependent upon the activation of P38 (Liu and Hofmann, 2004). Furthermore, the phosphorylation status of ERK1/2 and P38 can be increased by H_2O_2 and As^{3+} respectively, both of which are linked to oxidative stress. The observation of a consistent nuclear accumulation of CAR during the decay of the p-ERK signal at the 2- and 4-hour time points suggests the reduction in ERK1/2 activity is sufficient to permit CAR activation, which occurs concurrently with the nuclear accumulation of P38/p-P38. In order for CAR to translocate to the nucleus, it must first be dephosphorylated by PP2A (Yoshinari et al., 2003) in order to interact with P38 to increase CAR's transactivation activity (Hori et al., 2016). Activated P38 phosphorylates CAR at the conserved Thr38 residue to export CAR from the nucleus. These changes in the phosphorylation status of

P38 and ERK1/2 were also observed in whole-cell lysate from a *hUGT1* adult time course (data not shown), supporting our hypothesis of the oxidative stress-MAPK-CAR axis.

It has been reported that intestinal differentiation and crypt formation involves ROS and the activation of P38 (Houde et al., 2001; Rodriguez-Colman et al., 2017). Intestinal maturation is essential to both nutrient uptake and metabolic waste/toxicant removal. From studies in *hUGT1* mice, early intestinal expression of UGT1A1 is important to metabolize bilirubin while hepatic UGT1A1 expression is developmentally delayed (Fujiwara et al., 2010). Maturation of intestinal epithelial cells can be estimated by the decreases in genes related to cell stemness and the increase of functional genes related to the differentiated cell types. For example, the brush border glucosidase known as sucrose isomaltase, SIS, is only expressed in maturing and mature duodenum and jejunum enterocytes (Rubino et al., 1964). Alternatively, the *Lrp2* gene encodes for a protein known as megalin, which mediates nutrient uptake by endocytosis, and it's expression in the jejunum and ileum is down regulated as those tissues develop (Vázquez-Carretero et al., 2014). These and other genes, like *Glb1* and *Krt20* are markers for intestinal maturation when down- and up-regulated, respectively (Chen et al., 2017). Intestinal maturation markers were examined and it was determined that low doses of Cd^{2+} may induce intestinal maturation as inferred by inhibition of the *Glb1* and *Lrp2* genes and the induction of the *Sis* and *Krt20* genes (**Fig. S3**). Recently, it was reported that the nuclear receptor corepressor 1 (NCoR1), which regulates CAR activity at the PBREM (Mäkinen et al., 2002), is also capable of regulating intestinal maturation (Chen et al., 2017). Intestinal epithelial cell specific knockout of NCoR1 leads to changes in maturation markers and induction of UGT1A1 similar to what we have observed. Thus, it may be

possible that Cd^{2+} cadmium inhibits NCoR1, which increases maturation and de-represses CAR's transcriptional activity.

The most obvious implication of the oxidative stress-MAPK-CAR signaling axis resides in changes of xenobiotic metabolism from pro-oxidant activation of CAR. This could impact therapeutic outcomes in patients exposed to environmental pro-oxidants, such as heavy metals from smoking or contaminated drinking water and soil, or from indirect antioxidants found in certain diets and commercial supplements. It is possible that future studies making use of RNA-seq, metabolomics, and exposure data may reveal a correlation between pro-oxidant, toxicant exposure, and an individual variability in xenobiotic metabolism stemming from CAR activity.

Acknowledgments

Author Contributions

Participated in research design: Paszek, Tukey

Conducted experiments: Paszek

Performed data analysis: Paszek

Wrote or contributed to the writing of the manuscript: Paszek, Tukey

References

Bonzo JA, Belanger A, and Tukey RH (2007) The role of chrysin and the Ah receptor in induction of the human UGT1A1 gene in vitro and in transgenic UGT1 mice. *Hepatology* **45:**349-360.

Bosma PJ, Seppen J, Goldhoorn B, Bakker C, Oude ER, Chowdhury JR, Chowdhury NR, and Jansen PL (1994) Bilirubin UDP-glucuronosyltransferase 1 is the only relevant bilirubin glucuronidating isoform in man. *J Biol Chem* **269:**17960-17964.

Burchell B, Coughtrie M, Jackson M, Harding D, Fournel-Gigleux S, Leakey J, and Hume R (1989) Development of human liver UDP-glucuronosyltransferases. *Dev Pharmacol Ther* **13:**70-77.

Chen S, Lu W, Yueh MF, Rettenmeier E, Liu M, Auwerx J, Yu RT, Evans RM, Wang K, Karin M, and Tukey RH (2017) Intestinal NCoR1, a regulator of epithelial cell maturation, controls neonatal hyperbilirubinemia. *Proc Natl Acad Sci U S A* **114:**E1432-E1440.

Chen S and Tukey RH (2018) Humanized UGT1 mice, regulation of UGT1A1,and the role of the intestinal tract in neonatal hyperbilirubinemia and breast milk induced jaundice. *Drug Metab Dispos*.

Chen S, Yueh MF, Bigo C, Barbier O, Wang K, Karin M, Nguyen N, and Tukey RH (2013) Intestinal glucuronidation protects against chemotherapy-induced toxicity by irinotecan (CPT-11). *Proc Natl Acad Sci U S A* **110:**19143-19148.

Chen S, Yueh MF, Evans RM, and Tukey RH (2012) The Pregnane-X-receptor controls hepatic glucuronidation during pregnancy and neonatal development in humanized UGT1 Mice. *Hepatology* **56:**658-667.

Fujiwara R, Nguyen N, Chen S, and Tukey RH (2010) Developmental hyperbilirubinemia and CNS toxicity in mice humanized with the UDP glucuronosyltransferase 1 (*UGT1*) locus. *Proc Natl Acad Sci U S A* **107:**5024-5029.

Honkakoski P, Moore R, Gynther J, and Negishi M (1996) Characterization of phenobarbital-inducible mouse *Cyp*2b10 gene transcription in primary hepatocytes. *J Biol Chem* **271:**9746-9753.

Hori T, Moore R, and Negishi M (2016) p38 MAP Kinase Links CAR Activation and Inactivation in the Nucleus via Phosphorylation at Threonine 38. *Drug Metab Dispos* **44:**871-876.

Houde M, Laprise P, Jean D, Blais M, Asselin C, and Rivard N (2001) Intestinal Epithelial Cell Differentiation Involves Activation of p38 Mitogen-activated Protein Kinase That Regulates the Homeobox Transcription Factor CDX2. *Journal of Biological Chemistry* **276:**21885-21894.

Koike C, Moore R, and Negishi M (2007) Extracellular signal-regulated kinase is an endogenous signal retaining the nuclear constitutive active/androstane receptor (CAR) in the cytoplasm of mouse primary hepatocytes. *Mol Pharmacol* **71:**1217-1221.

Liu M, Chen S, Yueh MF, Fujiwara R, Konopnicki C, Hao H, and Tukey RH (2016) Cadmium and arsenic override NF-kappaB developmental regulation of the

intestinal UGT1A1 gene and control of hyperbilirubinemia. *Biochem Pharmacol* **110-111:**37-46.

Liu Q and Hofmann PA (2004) Protein phosphatase 2A-mediated cross-talk between p38 MAPK and ERK in apoptosis of cardiac myocytes. *American Journal of Physiology-Heart and Circulatory Physiology* **286:**H2204-H2212.

Mäkinen J, Frank C, Jyrkkärinne J, Gynther J, Carlberg C, and Honkakoski P (2002) Modulation of Mouse and Human Phenobarbital-Responsive Enhancer Module by Nuclear Receptors. *Molecular Pharmacology* **62:**366.

McMahon M, Itoh K, Yamamoto M, Chanas SA, Henderson CJ, McLellan LI, Wolf CR, Cavin C, and Hayes JD (2001) The Cap'n'Collar basic leucine zipper transcription factor Nrf2 (NF-E2 p45-related factor 2) controls both constitutive and inducible expression of intestinal detoxification and glutathione biosynthetic enzymes. *Cancer Res* **61:**3299-3307.

Moi P, Chan K, Asunis I, Cao A, and Kan YW (1994) Isolation of NF-E2-related factor 2 (Nrf2), a NF-E2-like basic leucine zipper transcriptional activator that binds to the tandem NF-E2/AP1 repeat of the beta-globin locus control region. *Proc Natl Acad Sci U S A* **91:**9926-9930.

Mutoh S, Sobhany M, Moore R, Perera L, Pedersen L, Sueyoshi T, and Negishi M (2013) Phenobarbital indirectly activates the constitutive active androstane receptor (CAR) by inhibition of epidermal growth factor receptor signaling. *Sci Signal* **6:**ra31.

Osabe M and Negishi M (2011) Active ERK1/2 Protein Interacts with the Phosphorylated Nuclear Constitutive Active/Androstane Receptor (CAR; NR1I3),

Repressing Dephosphorylation and Sequestering CAR in the Cytoplasm. *Journal of Biological Chemistry* **286:**35763-35769.

Pearson HA (1967) Life-span of the fetal red blood cell. *The Journal of Pediatrics* **70:**166-171.

Ratman D, Vanden Berghe W, Dejager L, Libert C, Tavernier J, Beck IM, and De Bosscher K (2013) How glucocorticoid receptors modulate the activity of other transcription factors: A scope beyond tethering. *Molecular and Cellular Endocrinology* **380:**41-54.

Rodriguez-Colman MJ, Schewe M, Meerlo M, Stigter E, Gerrits J, Pras-Raves M, Sacchetti A, Hornsveld M, Oost KC, Snippert HJ, Verhoeven-Duif N, Fodde R, and Burgering BM (2017) Interplay between metabolic identities in the intestinal crypt supports stem cell function. *Nature* **543:**424-427.

Rubino A, Zimbalatti F, and Auricchio S (1964) Intestinal disaccharidase activities in adult and suckling rats. *Biochimica et Biophysica Acta (BBA) - Specialized Section on Enzymological Subjects* **92:**305-311.

Senekeo-Effenberger K, Chen S, Brace-Sinnokrak E, Bonzo JA, Yueh MF, Argikar U, Kaeding J, Trottier J, Remmel RP, Ritter JK, Barbier O, and Tukey RH (2007) Expression of the Human UGT1 Locus in Transgenic Mice by 4-Chloro-6-(2,3-xylidino)-2-pyrimidinylthioacetic Acid (WY-14643) and Implications on Drug Metabolism through Peroxisome Proliferator-Activated Receptor α Activation. *Drug Metabolism and Disposition* **35:**419-427.

Shin S, Wakabayashi N, Misra V, Biswal S, Lee GH, Agoston ES, Yamamoto M, and Kensler TW (2007) NRF2 Modulates Aryl Hydrocarbon Receptor Signaling: Influence on Adipogenesis. *Molecular and Cellular Biology* **27:**7188.

Sugatani J, Kojima H, Ueda A, Kakizaki S, Yoshinari K, Gong QH, Owens IS, Negishi M, and Sueyoshi T (2001) The phenobarbital response enhancer module in the human bilirubin UDP-glucuronosyltransferase UGT1A1 gene and regulation by the nuclear receptor CAR. *Hepatology* **33:**1232-1238.

Timsit YE and Negishi M (2014) Coordinated Regulation of Nuclear Receptor CAR by CCRP/DNAJC7, HSP70 and the Ubiquitin-Proteasome System. *PLOS ONE* **9:**e96092.

Vázquez-Carretero MD, Palomo M, García-Miranda P, Sánchez-Aguayo I, Peral MJ, Calonge ML, and Ilundain AA (2014) Dab2, Megalin, Cubilin and Amnionless Receptor Complex Might Mediate Intestinal Endocytosis in the Suckling Rat. *Journal of Cellular Biochemistry* **115:**510-522.

Yoda E, Paszek M, Konopnicki C, Fujiwara R, Chen S, and Tukey RH (2017) Isothiocyanates induce UGT1A1 in humanized UGT1 mice in a CAR dependent fashion that is highly dependent upon oxidative stress. *Scientific Reports* **7:**46489.

Yoshinari K, Kobayashi K, Moore R, Kawamoto T, and Negishi M (2003) Identification of the nuclear receptor CAR:HSP90 complex in mouse liver and recruitment of protein phosphatase 2A in response to phenobarbital. *FEBS Letters* **548:**17-20.

Yueh MF, Bonzo JA, and Tukey RH (2005) The role of Ah receptor in induction of human UDP-glucuronosyltransferase 1A1. *Methods Enzymol* **400:**75-91.

Yueh MF, Chen S, Nguyen N, and Tukey RH (2017) Developmental, Genetic, Dietary, and Xenobiotic Influences on Neonatal Hyperbilirubinemia. *Mol Pharmacol*.

Yueh MF and Tukey RH (2007) Nrf2-Keap1 Signaling Pathway Regulates Human *UGT1A1* Expression in Vitro and in Transgenic UGT1 Mice. *J Biol Chem* **282:**8749-8758.

Footnotes

This work was supported by U.S. Public Health Service Grants from the National Institute of Environmental Health Sciences [ES010337], General Medicine [GM126074] and the UCSD Graduate Training Program in Cellular and Molecular Pharmacology [GM007752].

DMD Fast Forward. Published on November 8, 2019 as DOI: 10.1124/dmd.119.089508
This article has not been copyedited and formatted. The final version may differ from this version.

Legends for Figures

Figure 1. NRF2-dependency of antioxidant response genes in neonatal *hUGT1* mice. Ten-day old *hUGT1/Nrf2*$^{+/+}$, *hUGT1/Nrf2*$^{+/-}$, and *hUGT1/Nrf2*$^{-/-}$ neonatal mice were treated with vehicle (blue circles) or Cd^{2+} (10 mg/kg od. po.) (red squares) for two days before collecting intestinal tissue for RT-qPCR analysis of oxidative stress markers. The genes examined include *Nqo1, Ho-1, Gsta1, Gsta2,* and *Gstm3*. (Mean +/- SEM, Two-way ANOVA; * P<0.05, *** P<0.001, **** P<0.0001)

Figure 2. Cd^{2+} reduces TSB levels in *hUGT1* neonatal mice in an NRF2 independent fashion. Ten-day old *hUGT1/Nrf2*$^{+/+}$, *hUGT1/Nrf2*$^{+/-}$, and *hUGT1/Nrf2*$^{-/-}$ neonatal mice were treated with vehicle (blue circles) or Cd^{2+} (10 mg/kg od. po.) (red squares) for two days before collecting blood and intestinal tissues. (A) Changes in TSB levels (mg/dL) from mice treated with Cd^{2+}. (B) Changes in the expression of the *UGT1A1* gene. (C) Changes in the expression of the UGT1A1 protein as visualized by Western blot analysis and quantified by normalizing to GAPDH expression and set relative to vehicle treated *hUGT1/Nrf2*$^{+/-}$ mice. (Mean +/- SEM, Two-way ANOVA; * P<0.05, ** P<0.01, **** P<0.0001)

Figure 3. NRF2-indendent changes of intestinal *Cyp2b10* gene expression and CAR localization. Ten-day old *hUGT1/Nrf2*$^{+/+}$, *hUGT1/Nrf2*$^{+/-}$, and *hUGT1/Nrf2*$^{-/-}$ neonatal mice were treated with vehicle (blue circles) or Cd^{2+} (10 mg/kg od. po.) (red squares) for two days before collecting intestinal tissues. (A) Changes in the expression of the

Cyp2b10 gene were observed by RT-qPCR. (B) Nuclear localization of CAR was determined by Western blot analysis of fractionated intestinal protein extracts. Expression of CAR was quantified by normalizing to HDAC-1 and set relative to vehicle treated *hUGT1/Nrf2*$^{+/-}$mice. (Mean +/- SEM, Two-way ANOVA; * P<0.05, ** P<0.01, *** P<0.001)

Figure 4. Changes in intestinal MAPK phosphorylation and CAR localization following Cd^{2+} treatment in *hUGT1* neonates. Twelve-day old neonatal *hUGT1* mice were treated with vehicle or Cd^{2+} (10 mg/kg po.) and intestinal tissues were collected 30, 60, 120, and 240 minutes after exposure. Intestinal protein extracts were fractionated into nuclear and cytosolic components, and changes in (A) nuclear P38 content and phosphorylation status, (B) cytosolic ERK1/2 content and phosphorylation status, and (C) CAR localization were visualized by Western blot analysis with H3 and tubulin for nuclear and cytoplasmic loading controls. Quantifications and statistical analyses for A, B, and C can be found in supplementary figures 4, 5, and 6, respectively.

Figure 5. Hepatic and intestinal induction of *UGT1A1* and *Cyp2b10* in *hUGT1/Nrf2* neonatal mice. Ten-day old *hUGT1/Nrf2* $^{+/-}$ and *hUGT1/Nrf2* $^{-/-}$ neonates were treated with vehicle (blue circles) or PEITC (200 mg/kg od. po.) (red squares) for two days before collecting liver and small intestine. Gene expression for *UGT1A1* and *Cyp2b10* in each tissue were examined by RT-qPCR. (Mean +/- SEM, Two-way ANOVA; * P<0.05, ** P<0.01, *** P<0.001, **** P<0.0001)

DMD Fast Forward. Published on November 8, 2019 as DOI: 10.1124/dmd.119.089508
This article has not been copyedited and formatted. The final version may differ from this version.

Tables

Table 1. Primers utilized for real-time PCR analysis of selected genes

Gene	Forward (5'→3')	Reverse (5'→3')
hUGT1A1	CCA TCA TGC CCA ATA TGG TT	CCA CAA TTC CAT GTT CTC CA
Cyp1a1	TGC CCT TCA TTG GTC ACA TG	CAC GTC CCC ATA CTG CTG ACT
Cyp2b10	AAG GAG AAG TCC AAC CAG CA	CTC TGC AAC ATG GGG GTA CT
Cyp3a11	ACA AAC AAG CAG GGA TGG AC	CCC ATA TCG GTA GAG GAG CA
Cyp4a10	CAC ACC CTG ATC ACC AAC AG	TCC TTG ATG CAC ATT GTG GT
Nqo1	TTT AGG GTC GTC TTG GCA AC	GTC TTC TCT GAA TGG GCC AG
Ho-1	ACA GGG TGA CAG AAG AGG CTA AGA C	ATT TTC CTC GGG GCG TCT CT
Gsta1	AGC CCG TGC TTC ACT ACT TC	TCT TCA AAC TCC ACC CCT GC
Gsta2	AAT CAG CAG CCT CCC CAA T	TCC ATC AAT GCA GCC ACA CT
Gstm3	AAA CCT GAG GGA CTT CCT GG	AAC ACA GGT CTT GGG AGG AA
Il-1b	GCA ACT GTT CCT GAA CTC AAC	ATC TTT TGG GGT CCG TCA ACT
Il-6	ACC AGA GGA AAT TTT CAA TAG GC	TGA TGC ACT TGC AGA AAA CA
Tnfα	GAT CGG TCC CCA AAG GGA TG	GGC TAC AGG CTT GTC ACT CG
Glb1	CAC TGC TGC AAC TGC TGG	ATG TAT CGG AAT GGC TGT CC
Lrp2	CCA GGA TTC TGG TGA TGA GG	CGG GAA CTC CAT CAC AAA CT
Krt20	CCT GCG AAT TGA CAA TGC TA	CCT TGG AGA TCA GCT TCC AC
Sis	ACC CCT AGT CCT GGA AGG TG	CAC ATT TTG CCT TTG TTG GAT GC
Cph	CAG ACG CCA CTG TCG CTT	TGT CTT TGG AAC TTT GTC TGC

DMD Fast Forward. Published on November 8, 2019 as DOI: 10.1124/dmd.119.089508
This article has not been copyedited and formatted. The final version may differ from this version.

Table 2. Antibodies utilized for Western blot analysis

Antibody	Supplier	Product #
Anti-mouse IgG, HRP-linked	Cell Signaling Technology	#7076
Anti-rabbit IgG, HRP-linked	Cell Signaling Technology	#7074
CAR	ABclonal	A1970
ERK1/2	Cell Signaling Technology	#9102
Phospho-ERK1/2	Cell Signaling Technology	#9101
GAPDH	Santacruz Biotechnology	sc-47724
HDAC-1	Santacruz Biotechnology	sc-6298
Histone 3	ABclonal	A2352
P38	Cell Signaling Technology	#9212
Phospho-P38	Cell Signaling Technology	#9211
Tubulin	Sigma-Aldrich	T9026
UGT1A1	Abcam	Ab170858

DMD Fast Forward. Published on November 8, 2019 as DOI: 10.1124/dmd.119.089508
This article has not been copyedited and formatted. The final version may differ from this version.

Figures

Figure 1

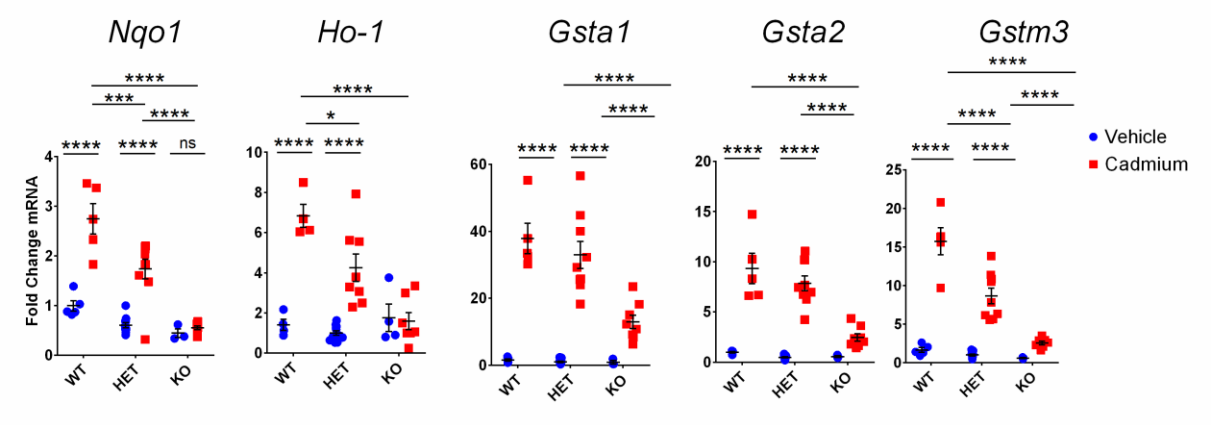

DMD Fast Forward. Published on November 8, 2019 as DOI: 10.1124/dmd.119.089508
This article has not been copyedited and formatted. The final version may differ from this version.

Figure 2.

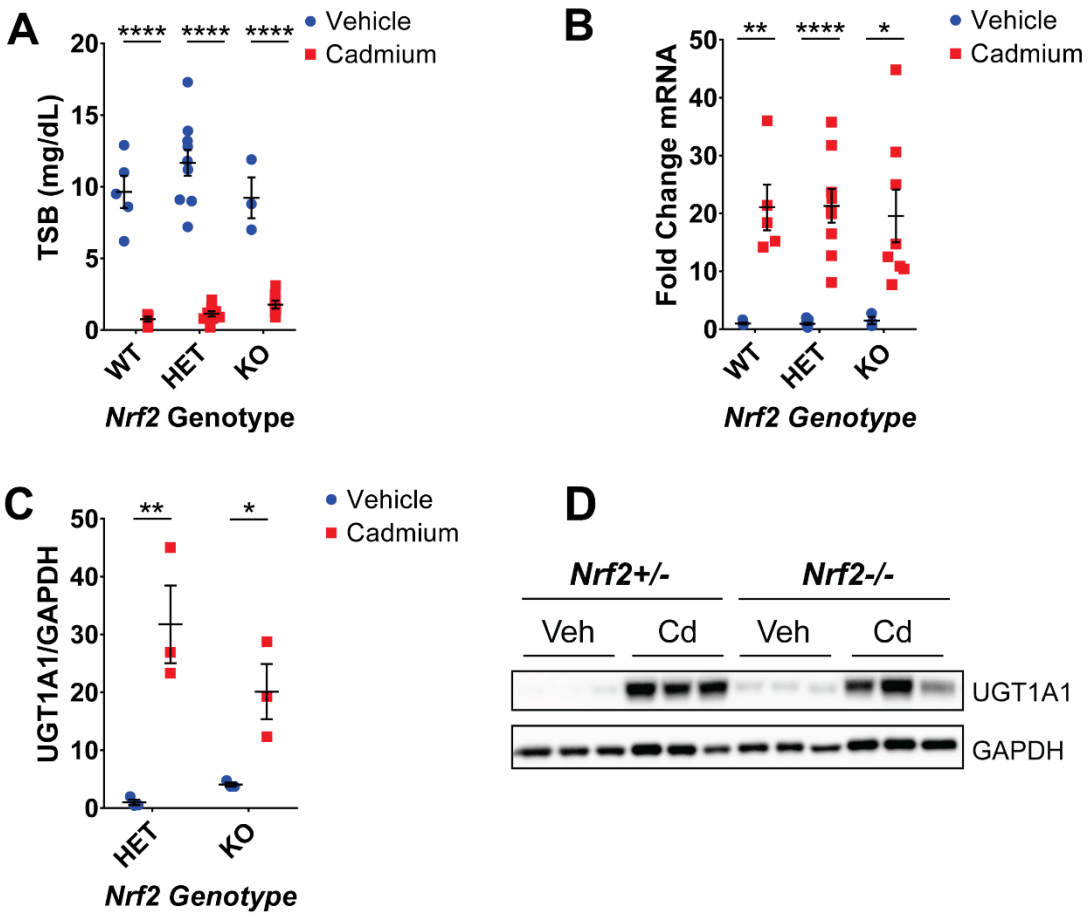

DMD Fast Forward. Published on November 8, 2019 as DOI: 10.1124/dmd.119.089508
This article has not been copyedited and formatted. The final version may differ from this version.

Figure 3.

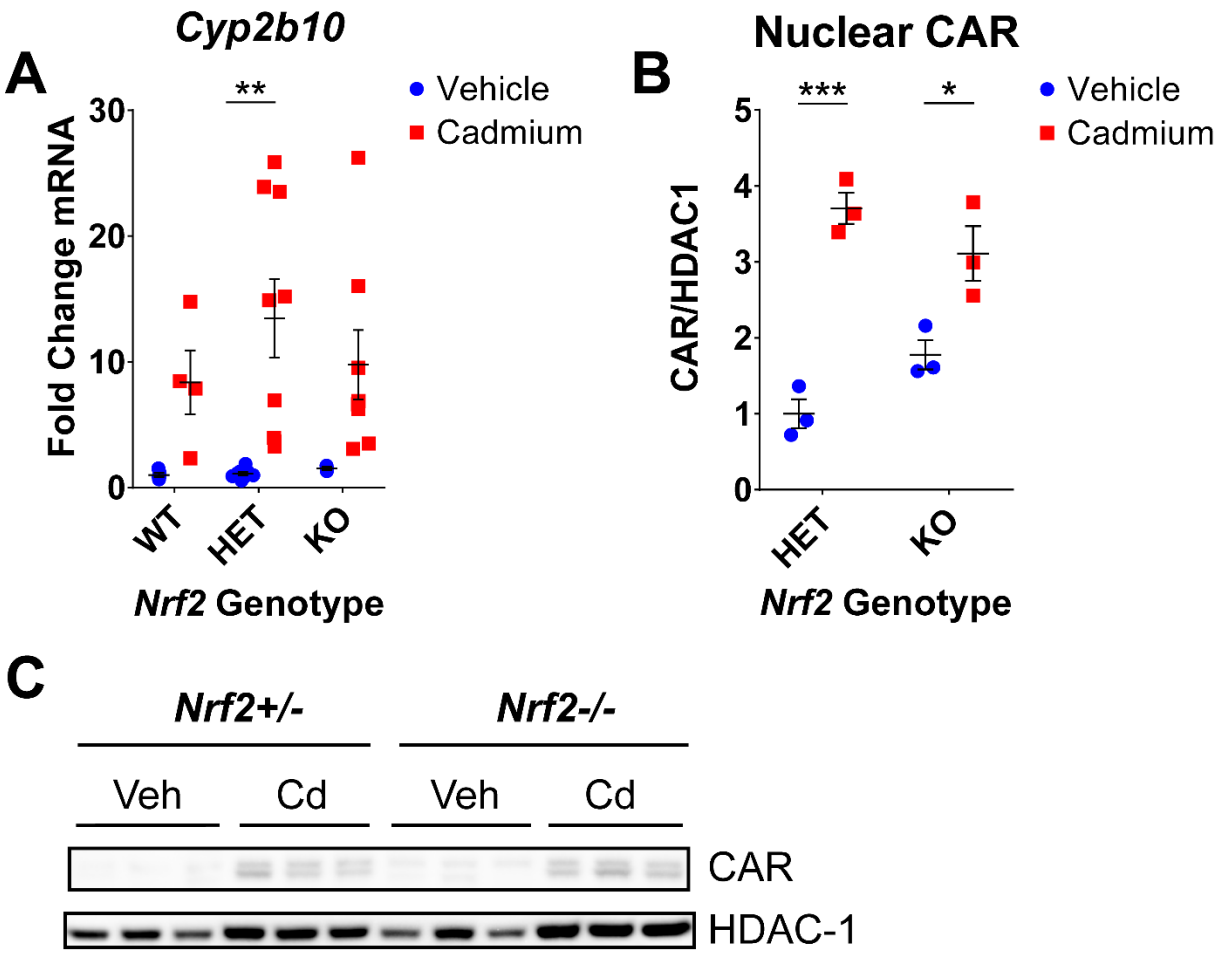

DMD Fast Forward. Published on November 8, 2019 as DOI: 10.1124/dmd.119.089508
This article has not been copyedited and formatted. The final version may differ from this version.

Figure 4.

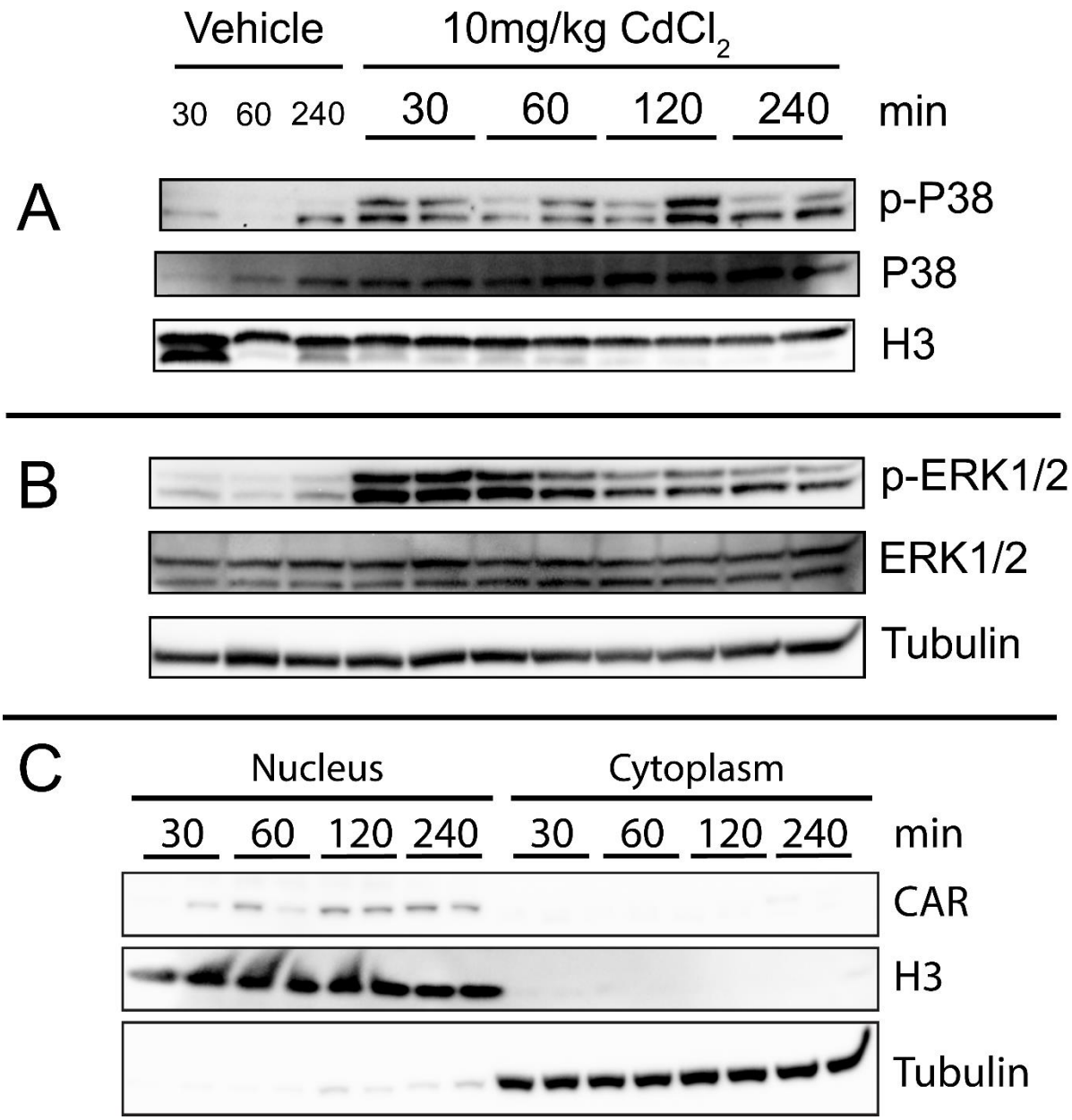

DMD Fast Forward. Published on November 8, 2019 as DOI: 10.1124/dmd.119.089508
This article has not been copyedited and formatted. The final version may differ from this version.

Figure 5.